Radiation Detection Technology and Methods (2020) 4:327–336
https://doi.org/10.1007/s41605-020-00187-9

ORIGINAL PAPER

Characteristics and time resolutions of two $CeBr_3$ gamma-ray spectrometers

Jianguo Qin[1] · Caifeng Lai[1] · Jun Xiao[1] · Xinxin Lu[1] · Tonghua Zhu[1] · Rong Liu[1] · Bangjiao Ye[2]

Received: 24 April 2020 / Revised: 6 June 2020 / Accepted: 19 June 2020 / Published online: 16 July 2020

Abstract

Purpose The purpose of this work is to study the pulse shape, energy resolution, non-proportionality of energy response for gamma-rays, and time characteristics of $CeBr_3$ detector.

Method The time and energy responses of two $CeBr_3$ detectors were characterized by an analog method and a digital method using a set of standard γ-ray sources. The pulse shape, energy resolution and non-proportionality (nPR) of energy response for γ-rays were characterized using the analog method. For the analog method, the high voltage applied to PMTs, parameters of walk and external delay of constant fraction discriminator were optimized. For the digital method, a CEAN 1729A digitizer with sampling frequency of 2 GS/s and resolution of 11 bit, and a digital constant fraction discrimination technique were used to study the time performance of the two $CeBr_3$ detectors. Then, the coincidence time resolutions of the $CeBr_3$ detectors for the gamma peaks of ^{22}Na and ^{60}Co were measured using the two methods.

Results The t_{rise}, lifetime τ, t_{fall} for $CeBr_3$ 21# and 22# are 11.2 ns, 23.8 ns, 50.2 ns, and 10.4 ns, 26.5 ns, 58.6 ns, respectively. The measured non-proportionality of $CeBr_3$ 21# and 22# are 1.08% and 2.22%, respectively. The time resolutions of the two $CeBr_3$ detectors are 244 ± 2 ps and 248 ± 3 ps at the energy peaks of ^{60}Co source, and 336 ± 2 ps and 335 ± 3 ps at 511 keV for the analog and the digital methods.

Conclusions The time resolutions obtained by the analog method and the digital method are almost identical. The $CeBr_3$ detector is a good option in the applications such as half-life measurements, ToF-PET and high counting rate conditions. Furthermore, it is a good γ-ray spectrometer owing to the preferable energy resolution and non-internal activity.

Keywords Cerium bromide · $CeBr_3$ · Time resolution · Analog and digital method · Non-proportionality

Introduction

Recently, some new inorganic scintillators with preferable performance have been produced, such as $LaBr_3/LaCl_3$, $CeBr_3$ and elpasolite crystal Cs_2LiYCl_6:Ce [1–5]. These scintillators are commonly used in γ-ray spectroscopy, nuclear physics research, astronomy and medical imaging, and they play an important role [6–9].

$CeBr_3$ and $LaBr_3$ both are attractive crystals with similar performance. The former promises to be an adequate substitute of the latter in some applications, because it has fast time response, high photon yield of 68,000 photons/MeV and more competitive price [10]. Practically, the energy resolution of $LaBr_3$ is a little better than $CeBr_3$. However, a major drawback of $LaBr_3$ is the intrinsic activity from ^{138}La, which produces 1.24 s^{-1} cm^{-3} as background in the energy range of 20–3000 keV [11, 12], while it is only about 0.04 s^{-1} cm^{-3} for $CeBr_3$ crystal [13, 14]. This could hamper its capability in detecting low-intensity γ-ray.

Furthermore, $CeBr_3$ crystal has slightly larger detection efficiency than $LaBr_3$, because the effective atomic number of $LaBr_3$ is 45.3 and density of which is 5.07 g/cm^3, while the values are 45.9 and 5.18 g/cm^3 for $CeBr_3$ crystal. More importantly, the pulse from $CeBr_3$ crystal not only has a fast rising time of about 0.5 ns, but also has a very short decay which characterized by a single component with about 20 ns in lifetime [4]. The performances of fast rise time and short fall time make it to be ideal for fast time and high count rate situations, and then, it can be used to measure the

✉ Jianguo Qin
stingg@126.com

1 Institute of Nuclear Physics and Chemistry, CAEP, P.O. Box 213, Mianyang 621900, China

2 Department of Modern Physics, University of Science and Technology of China, Heifei 230026, China

nuclear level lifetimes accurately [15]. Now $CeBr_3$ is promising to be a preferable substitute under the comprehensive consideration.

The delayed coincidence technique based on standard NIM electronics is commonly used to measure the time resolution of $CeBr_3$ crystal, which was referred to as an analog method. For this method, the parameters, such as walk and external delay time, must be optimized iteratively, and the processes are fussy and time-consuming. Accordingly, the digital method is used widely in waveform capturing [16–20], and it has the characteristics such as concise, higher efficiency, flexible and lower cost. As a result, a digital method was used to measure the time resolution of $CeBr_3$ detector in this work, and it was compared with the analog method.

In this work, the time resolutions of two $CeBr_3$ detectors were measured using both an analog method and a digital method for the gamma peaks of ^{22}Na and ^{60}Co. The energy response, energy resolution and non-proportionality of the energy response for γ-rays were characterized using the analog method, and the nanosecond-order half-life of ^{152}Sm 2^+ isomer was also measured directly.

Experimental specifications

$CeBr_3$ detectors

Two $CeBr_3$ crystals with the same dimension were manufactured by Beijing Glass Research Institute, and they are labeled as $CeBr_3$ 21$^{\#}$ and $CeBr_3$ 22$^{\#}$, respectively. The cylindrical crystals were all in 1″ × 1″, and they were wrapped with reflector material and sealed in an aluminum case. The crystals were optically coupled with a photon multiplier tubes (PMT) using viscosity silicon grease.

The PMTs labeled as CR173-01 were produced by HAMAMATSU. There are 8 dynodes and one entrance window of 1.5″ in diameter in the PMTs and only one output signal from the anode of the detectors. For the PMTs, the typical rising time is about 5 ns, the dark current is 2 nA at 1000 V, and the max high voltage is less than 1500 V [21].

Experimental setup

An analog method and a digital method were used to measure the time resolution of $CeBr_3$ detectors. For the analog method, the delayed coincidence technique [15] was used. The measurements of time resolution were taken with ^{22}Na and ^{60}Co γ-ray sources which positioned between CeBr3 21$^{\#}$ and 22$^{\#}$. Both the back-to-back positioned detectors were coupled to standard NIM front-end electronics as shown in Fig. 1a.

Since the detectors provided only one output signal, which is taken from the anode, the signals were split into two outputs with MT050 splitters. This is necessary to enable it to measure both time and energy characteristics simultaneously in one coincidence experiment. One output was connected to an ORTEC 584 constant fraction discrimination (CFD) module for the time measurement, while the other output was fed into an ORTEC 572A spectroscopy amplifier for selecting the coincidence energy window. The coincidence events were selected by an ORTEC 850 single channel analyzer (SCA) and ORTEC 418 coincidence unit based on the energy spectra from 572 A, and it was used as a gate for the time measurement.

Apart from the time resolution of $CeBr_3$ detectors, the energy response, energy resolution and non-proportionality of the energy response for γ-ray were also measured using the standard NIM electronics. To measure the energy characteristics more accurately, the output signals from detectors were firstly send to an ORTEC 113 preamplifier (not shown in Fig. 1), and they are fed into an ORTEC 572A amplifier subsequently.

For the digital method, a CAEN 1729A digitizer was used to substitute the analog modules except the coincidence unit *ORTEC* CO 4020 and splitter MT050. The output signals were split into two chains by MT050. One was send to a CO 4020 for coincidence with the signal of the other $CeBr_3$ detector, and the other split signal was fed into the digitizer to acquire the waveform data directly. The coincidence signal from CO 4020 was send into the digitizer as a trigger in order to decrease the memory burden of the personal computer. The time and energy information was analyzed offline.

A set of standard γ-ray sources produced by *AEA Technology* was used to determine the energy resolution, time resolution, photon non-proportionality and ^{152}Sm 2^+ isomer half-life as listed in Table 1 [22].

Energy response and resolution

The interaction between the incident photons and the crystal is mainly photoelectric effect, Compton scattering and pair production (when $E_\gamma \gg 1.02$ MeV). The energy of the Compton scattered photons $E_{\gamma'}$ and recoil electron E_e can be represented by Eqs. (1) and (2), where m_0, c and θ are the electron static mass, light speed in vacuum and the scattering angle of photon, respectively.

$$E_{\gamma'} = \frac{E_\gamma}{1 + \frac{E_\gamma}{m_0 c^2}(1 - \cos\theta)} \tag{1}$$

$$E_e = \frac{E_\gamma^2(1 - \cos\theta)}{m_0 c^2 + E_\gamma(1 - \cos\theta)} \tag{2}$$

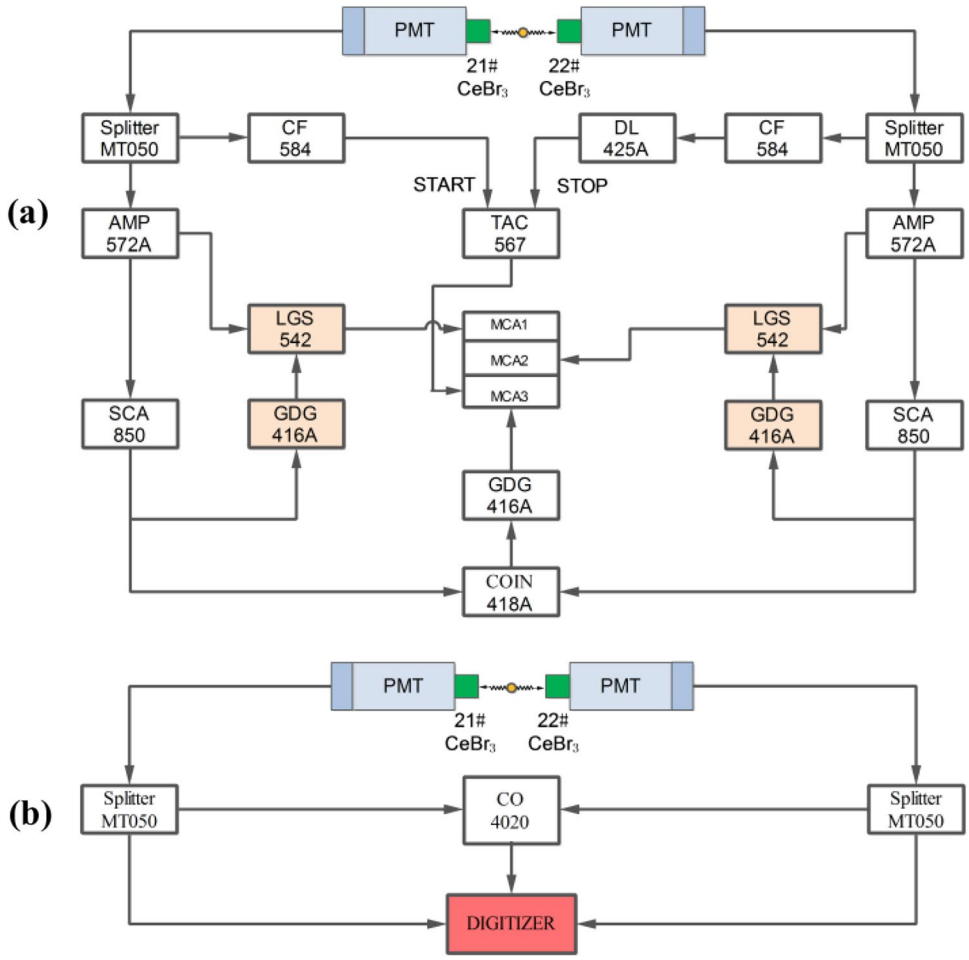

Fig. 1 Schematics of the coincidence time-delayed setup used to measure time response of the two $CeBr_3$ detectors. **a** Based on standard NIM electronics; **b** based on a digitizer. The standard NIM electronics were manufactured by *ORTEC*

Table 1 Standard γ-ray sources used for the characterization of the $CeBr_3$ detectors as indicated by asterisks

Nuclide	Energy resolution	nPR	Time resolution	Isomer half-life
^{22}Na		*	*	
^{241}Am		*		
^{60}Co	*	*	*	
^{133}Ba	*	*		
^{137}Cs	*	*		
^{152}Eu	*	*		*
^{226}Ra	*	*		
^{109}Cd	*	*		

The asterisk indicates that it has been applied in the corresponding test item

The energy deposition of photons formed a pulse height spectrum according to the processes mentioned above. The full energy (FE) peak, Compton edge (CE) and backscattering peak (BSP) can be identified clearly as the high energy resolution of $CeBr_3$ detectors. The CE peak and BSP peak of 511 keV, 1173.2 keV and 1332.3 keV are listed in Table 2. The energy resolution is determined by the ratio of the FWHM to the full energy peak, even though the real value of FWHM should be calibrated using the method shown in Ref. [10] for the non-proportionality.

Table 2 Energies of full energy peak, Compton edge and backscattering peak of 511 keV, 1173.2 keV and 1332.3 keV γ-rays

FE (keV)	CE (keV)	BSP (keV)
511	341.7	170.3
1173.2	963.2	209.8
1332.3	1117.6	214.4

Scintillation non-proportionality of response (nPR)

Scintillators have an intrinsic non-proportionality response between scintillator light yield and photon deposition which affects their energy resolution. The origin of nPR

in scintillator is extremely complex, and it can be affected by chemical composition, dopants, rare earth–cation substitution effect and anion effect [23–25]. According to the previous efforts in both experimental and theoretical modeling [14, 26], the nPR can be explained as that it originates from the nonlinear interactions of electrons and holes in a tiny excitation volume leading to a quenching of luminescence[25].

Gamma-ray non-proportionality can be traced back experimentally. Following the ideas of Pieter Dorenbos[27] and Wahyu Setyawan [23], the degree of photon nPR can be quantified by Eq. (3) [24], where $E_{max} = 662$ keV, $E_{min} = 22$ keV, $f_{nPR}(E_{max}) = 100\%$ and $f_{nPR}(E)$ is the value of nPR at the excitation energy E.

$$\sigma_{nPR} = \frac{1}{E_{max} - E_{min}} \int_{E_{min}}^{E_{max}} \left| f_{nPR}(E_{max}) - f_{nPR}(E) \right| dE \quad (3)$$

Time resolution and optimization

Time resolution with analog method

The measurements of time resolution were taken with ^{22}Na and ^{60}Co sources, which provide back-to-back 511 keV coincidence photons from positron annihilation and the cascade radiations from the 4^+ to 2^+ and 2^+ to 0^+ of ^{60}Ni isomer with a 0.71 ps half-life. In the case of ^{22}Na source, events that were recorded by $CeBr_3$ 21$^\#$ (511 keV) and 22$^\#$ (511 keV) formed a time spectrum, and the time spectrum was gated by events in the peak of 511 keV. The both energy gates were set at FWHM of the photopeaks.

In the case of ^{60}Co source, the 1173.2 keV and 1332.3 keV photopeaks were recorded in each detector. The time resolution represents an average value for the two possible situations. In the first step, the time spectrum for $CeBr_3$ 21$^\#$ (1173.2 keV) and 22$^\#$ (1332.3 keV) was recorded; then, a second time spectrum for $CeBr_3$ 21$^\#$ (1332.3 keV) and 22$^\#$ (1173.2 keV) was created. The energy gates were set roughly at FWHM of the photopeaks. The final time resolution FWHM was given by the summed time spectrum.

The time resolution as a function of high voltage on PMTs, external delay and CFD walk was measured to find the optimal time resolution, and the optimization processes were iterated. Based on the measurements, the best conditions of walk, external delay and high voltage have been optimized, and then, we have got the optimal time resolution.

The ADC for recording time spectra were calibrated by signals from ORTEC 462 time calibrator; the result is 3.254 ± 0.003 ps/Channel. Furthermore, the upper limit of intrinsic time resolution 25.7 ps of the NIM electronics was obtained simultaneously using the simultaneous signals that produced by ORTEC 462 module.

Time resolution with digital method

The schematic circuit of digital method is shown in Fig. 1b; the signal recording length, resolution and sampling frequency of CAEN 1729A digitizer are 500 ns, 11 bit and 2 GS/s, respectively. The acceptable input range is $-0.5 \sim 0$ V. Data are transferred to the main acquisition system via VME bus and then could be read by a V1718 controller and be send to the acquisition system via a USB line.

As same as in analog method, ^{22}Na and ^{60}Co sources were used to measure the time resolution with digital method. Waveforms of all the coincidence events of $CeBr_3$ 21$^\#$ and 22$^\#$ were recorded event by event. In order to obtain the optimal time resolution, there are two steps must be performed: One is timing the waveform, and the other is the optimization of energy window.

In step one, a digital constant fraction discrimination (dCFD) method [28] based on C language was used to timing the waveforms. The time resolution of 511 keV and 1173.2 keV/1332.3 keV was investigated to find the optimal conditions. Furthermore, the amplitude of waveforms was picked up, and then, the time and amplitude of $CeBr_3$ 21$^\#$ and 22$^\#$ reformed a pair of coincidence events for further analysis.

Secondly, the coincidence events were discriminated via energy windows, and the energy windows of 511 keV, 1173.2 keV and 1332.3 keV are equal to the FWHM of corresponding photopeaks as same as in analog method. Finally, the optimal time resolution for ^{22}Na and ^{60}Co sources was obtained using MATLAB tools.

Results and discussion

The output pulse shape of PMT

Pulse waveforms were collected from anode output of detectors for ^{137}Cs source using a Tektronix TDS7254 digital phosphor oscilloscope at a sampling rate of 2.5 GS/s. Based on the analysis of about one hundred waveforms of 662 keV γ-rays, a typical pulse shape from the detectors was obtain. The measured pulses of $CeBr_3$ 21$^\#$ and 22$^\#$ detectors are shown in Fig. 2. Pulse rise time t_{rise} represents the time when the pulse amplitude changes from 10 to 90% of the maximum value. On the contrary, pulse decay time t_{fall} represents the time when the pulse amplitude changes from 90% of the maximum value to 10%. The exponential decay function is used to fit the falling part of the pulse, and the decay constant is defined as the lifetime τ.

According the measured result, the rise time t_{rise}, lifetime τ and decay time t_{fall} of the signals from $CeBr_3$ 21$^\#$ anode are 11.2 ns, 23.8 ns and 50.2 ns, while those from $CeBr_3$ 22$^\#$ are

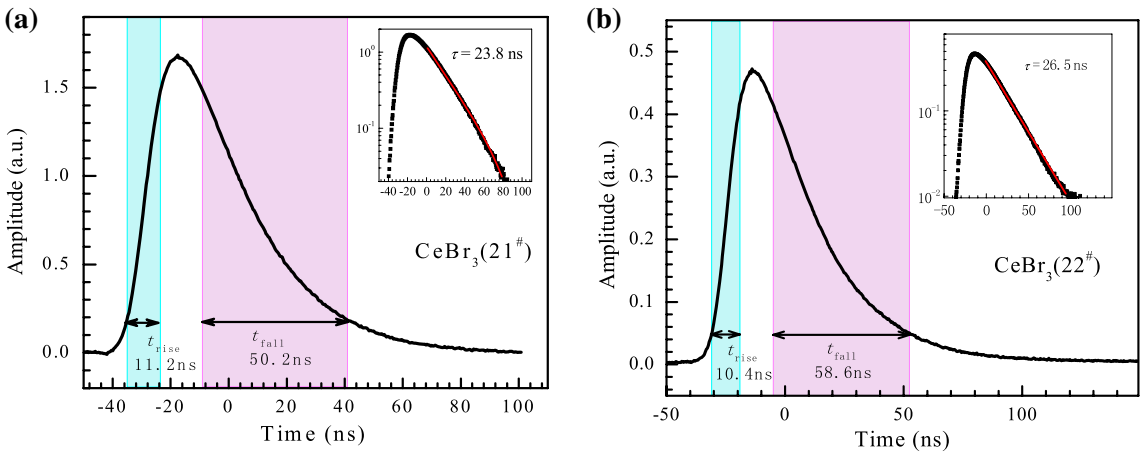

Fig. 2 PMT output pulses (inverted for display) from $CeBr_3$ detectors, **a** 21#, **b** 22#. The inner figures are the same data as the outer figures with a logarithmic scale of *Y*-axis, which fitted by a exponential decay function

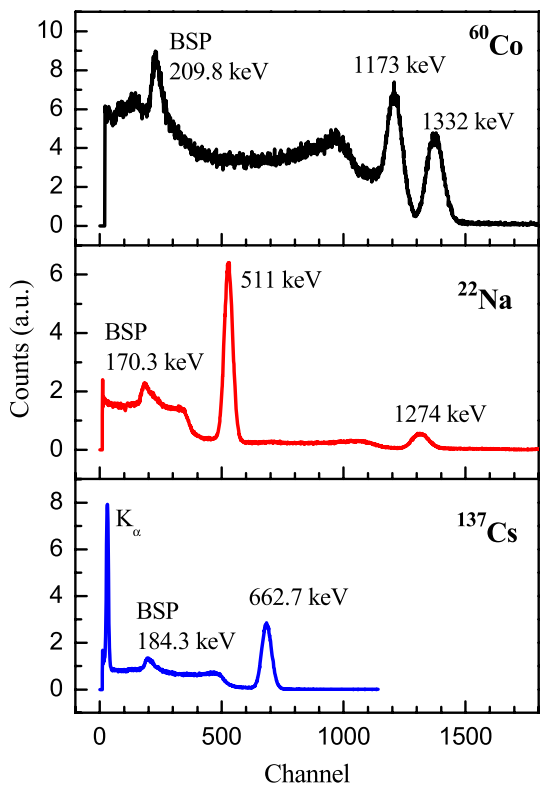

Fig. 3 Gamma-ray responses of $CeBr_3$ 22# detector at HV = 1050 V based on analog method; for the ^{60}Co, ^{22}Na and ^{137}Cs sources, the $CeBr_3$ 21# has similar results with a poorer energy resolution

10.4 ns, 26.5 ns and 58.6 ns, respectively. The fitted lifetimes for $CeBr_3$ 21# and 22# are roughly consistent with the lifetime of the 5d → 4f transition of Ce^{3+} [29] and the lifetime of 23.9 ns from N. D'olympia [15]. Nevertheless, the most important factor for time resolution measurement lies in that the rise time of $CeBr_3$ 21# and 22# is both much longer than the typically value of 0.4–2 ns in references [10, 15, 30]. It is a unfavorable factor for measuring time resolution.

Energy resolution and nPR

The typical energy spectra of ^{60}Co, ^{22}Na and ^{137}Cs sources obtained by $CeBr_3$ 22# detector with working voltage of 1050 V are plotted in Fig. 3. The shaping time, capacitance and gain of the ORTEC 572A spectroscopic amplifier were 3 μs, 500 pF and 10, respectively. The ratio of peak to Compton continuum is 4 for ^{137}Cs source, while $CeBr_3$ 21# has a similar γ-ray response with a poorer energy resolution.

The energy resolution (FWHM/E_0 %) of $CeBr_3$ 21# and 22# has been measured with six radioactive sources, as listed in Table 1. Energy resolutions as a function of incident γ-ray energy for the two $CeBr_3$ detectors are shown in Fig. 4, and the energy resolutions for $CeBr_3$ 21# and 22# are 6.4% and 5.2% at 662 keV of ^{137}Cs source. The measured value is bigger than the typically value of 4–5.1% [13, 31], especially for $CeBr_3$ 21# detector. This is due to the gluing process in crystal manufacturing and also affected partially by the PMTs used in this work. The lines in Fig. 4 are nearly exact the fitting functions of $1/\sqrt{E}$.

The measurements of nPR response for $CeBr_3$ 21# and 22# with standard radioactive γ-ray source are shown in Fig. 5. The nPR curve is usually characterized by a lowest value of nPR at the lowest energies, a K-dip in the nPR curve near K-shell absorption edges of cerium and bromine, and a smooth monotonic increase in the nPR curve with increasing photon energy up to 662 keV. Curves in Fig. 5 are normalized to 1 at 662 keV. The nPR of I.V. Khodyuk [24] is 2.42% from 10 to 662 keV, and the experiment was carried out on a synchrotron radiation facility that provide monochromatic X-ray beam. The nPR of Kanai S. Shah [32] is 4% from

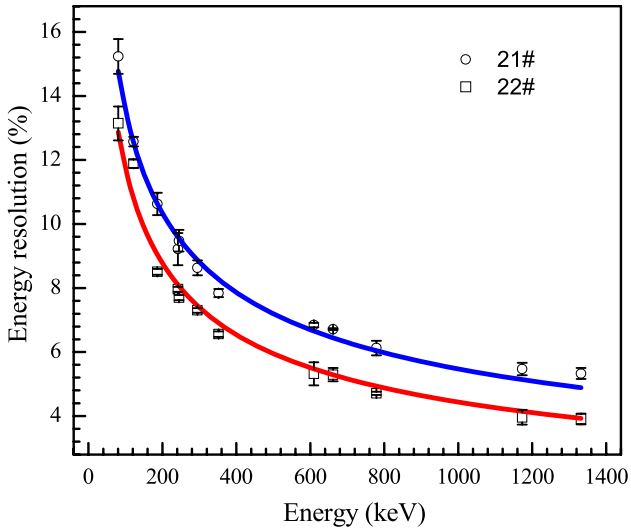

Fig. 4 Energy resolution FWHM as function of γ-ray energy for $CeBr_3$ 21# and 22# detectors based on analog method. The lines are the best fitting functions of $1/\sqrt{E}$

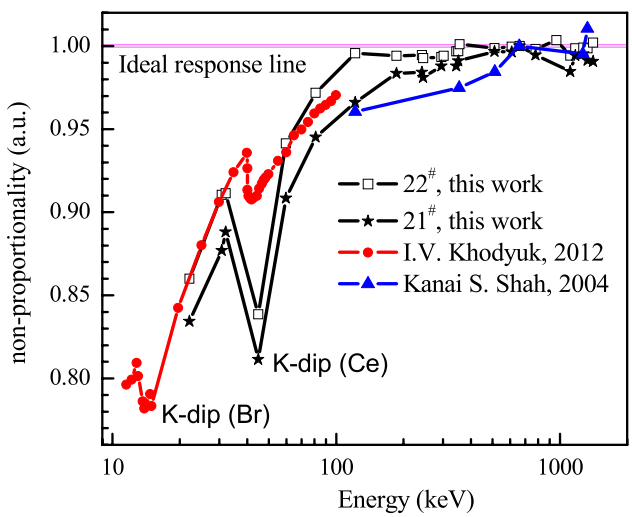

Fig. 5 nPR response of $CeBr_3$ detectors measured with standard radioactive γ-ray sources

100 to 1275 keV. In the energy region from 22 to 662 keV, the measured nPR of $CeBr_3$ 21#, 22# are 2.22% and 1.08%, respectively. Poorer energy resolution of $CeBr_3$ 21# can be attributed to the higher degree of nPR.

Time resolution

Time resolution using analog method

As discussed in "time resolution with analog method" in section, the time resolution strongly depends on those three factors, especially the applied high voltage and external

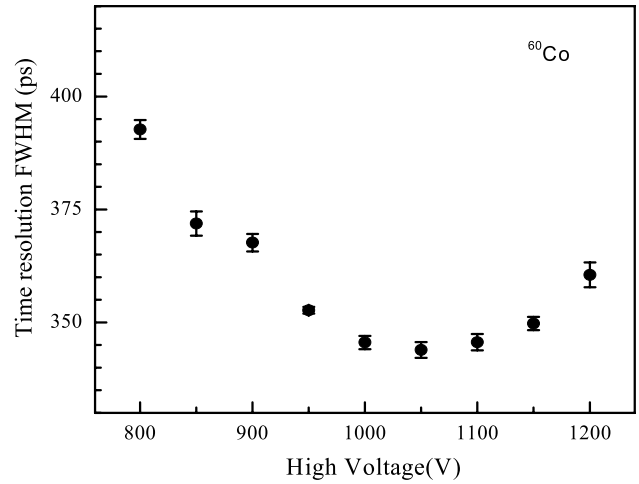

Fig. 6 Relation of time resolution FWHM as a function of high voltage value for an individual $CeBr_3$ detector using the ^{60}Co source

delay. So the iterative and optimization process should have been done before the system being applied in measurements. Firstly, the walk of CFD modules was optimized one by one. The result shows that there is an appropriate range in which the walk has a little influence to measurements.

Secondly, using ^{60}Co source, we have measured the time resolution as a function of the high voltage applied to PMTs; the results are shown in Fig. 6. The time resolution steadily improves, while the voltage increases up to 1050 V with the minimum value of 345 ps and then degrades slightly. This can be explained that the signal-to-noise ratio (SNR) is improved with the high voltage increasing, and then, a good SNR is in favor of the time resolution. Meanwhile, space-charge effects will degrade the pulse shape from PMT with the further increased high voltage, and then, the degraded pulses lead to a worse time resolution.

Finally, based on these results we have measured the time resolution as a function of the external CFD delay time applied to the detector system. The measured results for ^{60}Co source are shown in Fig. 7. The time resolution steadily improves with the external delay time t_d increasing up to 6 ns and then remains rather steady with the minimum value of about 345 ps when t_d varies from 6 to 12 ns, and then degrades along with the increasing t_d.

For ORTEC 584 CFD, the constant fraction factor $f = 0.2$ was set in factory and was used in this work. Theoretically, for ideal triangular input signals, the recommended decay is $t_d = 1.1t_r - 0.8$ ns, where f and t_r are the attenuated factor and rise time of the input signal from 10 to 90%, respectively. Thus, the recommended t_d for CFDs with $CeBr_3$ 21# and 22# is 11.5 and 10.6 ns, respectively. It is roughly consistent with experimental result.

According to the iterative optimization processes mentioned above, the optimal measuring conditions are $t_d = 10$ ns

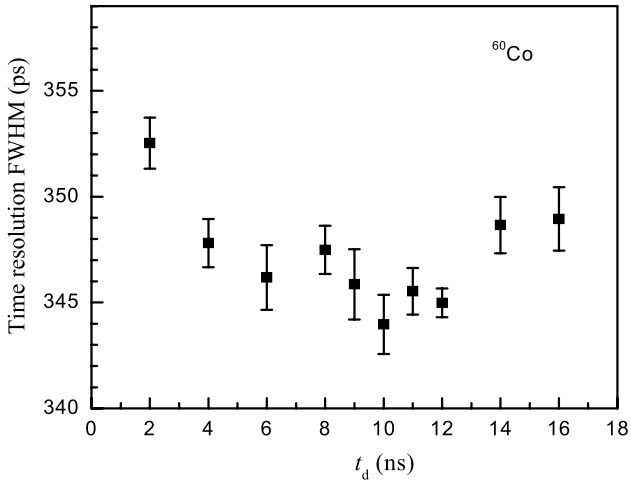

Fig. 7 Relation of time resolution FWHM as a function of external delay time for an individual CeBr3 detector using the ^{60}Co source

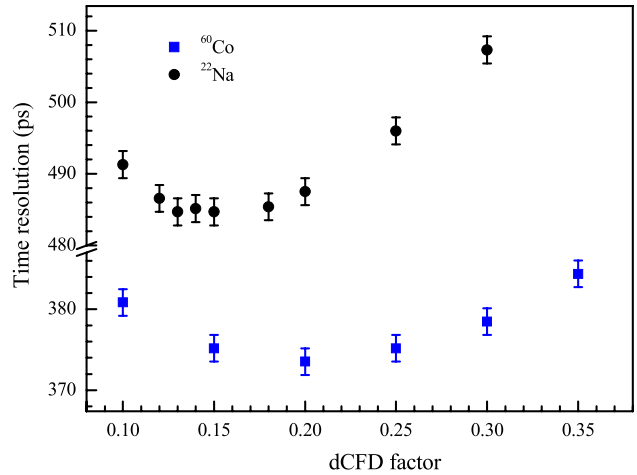

Fig. 9 Time resolution as a function of dCFD factor for ^{22}Na and ^{60}Co sources

and HV = 1050 V. The time resolutions for $CeBr_3$ 21# and 22# at energies of ^{22}Na and ^{60}Co sources using the analog method are plotted in Fig. 8a and b. The optimal time resolutions FWHM are 475 ps and 344 ps. Both the time spectra were obtained by selecting the events with energy range in the FWHM of corresponding photopeaks. In the case of ^{60}Co source, the time resolution represents an average value for two possible situations as mentioned in "time resolution with analog method" in section.

The measured time resolutions involve contributions of the intrinsic time resolution 25.7 ps of NIM electronics and that of detectors $CeBr_3$ 21# and $CeBr_3$ 22#. The relation of time resolution and the contributors can be expressed as $T_{total} = (T^2_{CeBr3\ 21\#} + T^2_{CeBr3\ 22\#} + T^2_{NIM})^{0.5}$. Here, $T_{CeBr3\ 21\#}$ and $T_{CeBr3\ 22\#}$ are both much larger than T_{NIM}, and the influence of T_{NIM} to T_{total} can be neglected (< 0.3%).

Assuming that both detectors are nearly identical, we could calculate the time resolution of a single $CeBr_3$ detector by dividing the FWHM value by $\sqrt{2}$. The time resolution of a single $CeBr_3$ detector with analog method at 511 keV and 1173 keV/1332 keV is 244 ps and 336 ps, respectively.

Time resolution using digital method

The dCFD factors were optimized before the system was applied to measure time resolution. The time resolution as a function of dCFD factor is shown in Fig. 9, and the optimal dCFD factors for ^{60}Co and ^{22}Na sources are 0.2 and 0.15, respectively. While dCFD factors in the range of 0.12–0.2

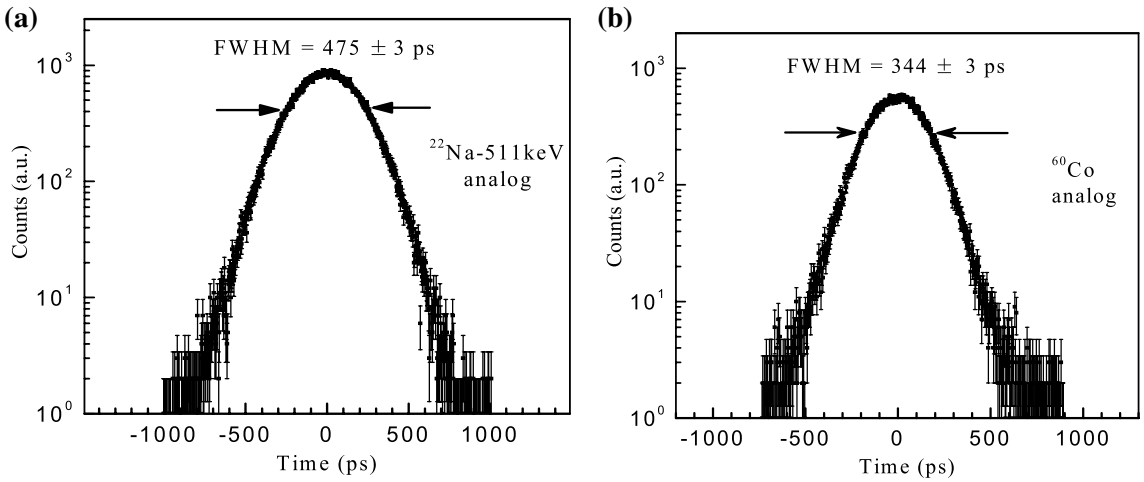

Fig. 8 Time resolutions for $CeBr_3$-HAMAMATSU PMT detectors (21# and 22#) in coincidence using analog method. The FWHM resolutions are obtained assuming the two detectors have the same time characteristics. **a** ^{22}Na source; **b** ^{60}Co source

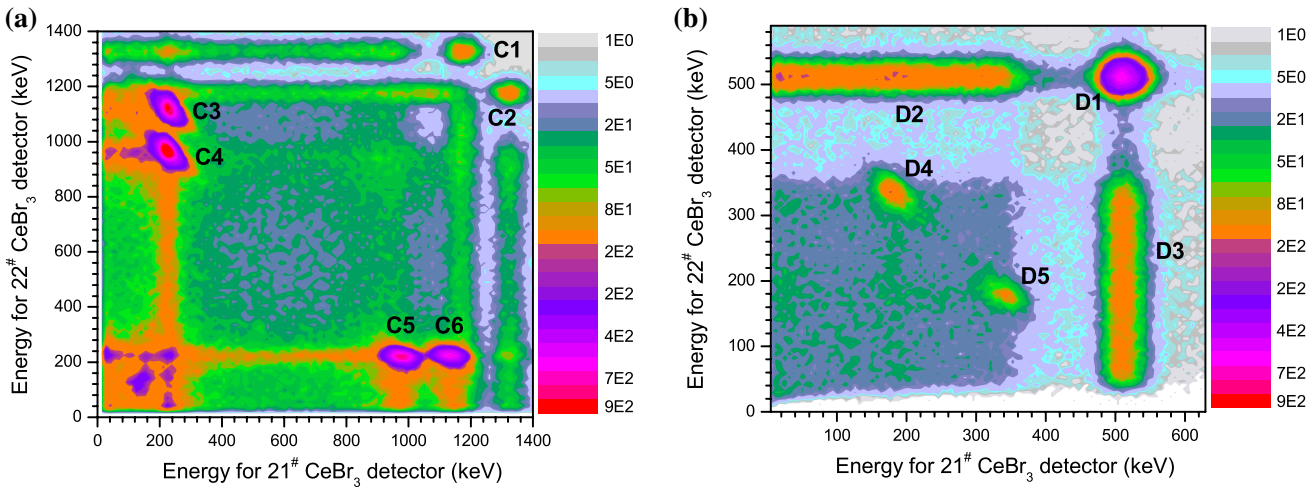

Fig. 10 2D energy spectra of coincidence events of $CeBr_3$ 21# and 22# detectors for ^{60}Co and ^{22}Na sources based on a *CAEN* 1729A digitizer, **a** ^{60}Co source; **b** ^{22}Na source

Table 3 Details of the coincidence events of $CeBr_3$ detectors for ^{60}Co and ^{22}Na sources; the meaning and energy value of abbreviations FE, CE and BSP are given in Table 2; FE (511) represents the full energy peak of 511 keV; BSP (^{60}Co) represents the backscattering peak of 1173 keV and 1332 keV

Item	Coincidence events of ^{60}Co		Item	Coincidence events of ^{22}Na	
	$CeBr_3$ 22#	$CeBr_3$ 21#		$CeBr_3$ 22#	$CeBr_3$ 21#
C1	FE (1332)	FE (1173)	D1	FE (511)	FE (511)
C2	FE (1173)	FE (1332)	D2	FE (511)	CE (511)
C3	CE (1332)	BSP (^{60}Co)	D3	CE (511)	FE (511)
C4	CE (1173)	BSP (^{60}Co)	D4	CE (511)	BSP (511)
C5	BSP (^{60}Co)	CE (1173)	D5	BSP (511)	CE (511)
C6	BSP (^{60}Co)	CE (1332)			

for ^{22}Na source, the time resolution remains rather steady with in one standard error, and the largest difference is less than 0.5%.

The time resolutions with the digital method at the peaks of ^{22}Na and ^{60}Co source were measured and analyzed after dCFD optimization process. The distribution of coincidence events are shown in Fig. 10. They are composed of mainly by all the coincidence events among the FE, CE and BSP, and the details of coincidence events are summarized in Table 3.

As shown in Fig. 10a, C1 and C2 are the valuable coincidence events with the energies of 1173.2 keV and 1332.3 keV of ^{60}Co source. Furthermore, the C3 and C4 are more clearly separated than C5 and C6, which represents $CeBr_3$ 22# detector has a better energy resolution than $CeBr_3$ 21#. For the case of ^{22}Na source as shown in Fig. 10b, besides the valuable coincidence events D1, coincidence events between the photopeak and the Compton edge (D2, D3) are notable. The intensity of the backscattering peaks and photopeaks for ^{60}Co is larger than ^{22}Na; this is caused by the different γ-γ angular correlation.

Based on the optimal dCFD factors, the coincidence time resolutions of $CeBr_3$ 21# and 22# detectors at the energy peaks of ^{60}Co and ^{22}Na sources were obtained with the digital method, as shown in Fig. 11. The time resolution of each $CeBr_3$ detector was calculated by the same method as used in the analog experiment, as listed in Table 4. The quoted errors in Table 4 include contributions from both the calibration constant and peak fitting.

Besides the high voltage applied to PMT, the input range, sample frequency and the resolution of the digitizer as well as the timing discrimination method are the main influence factors to time resolution [28, 33]. For the digitizer CAEN 1729A used in this work, the input range is inadequate. Otherwise, the time resolution can be better.

Comparing the analog and the digital method used in this work, the advantage of the latter is no need to adjust the parameters of electronics, while the disadvantage is the influence by the performance of digitizer. From Table 4, we can see that the measured results are nearly identical with these two methods. It shows that the digital method based on digitizer at the present time can reach the level of analog method or even better than the latter. Furthermore, it can be conclude that time resolution will be much improved hopefully, if the PMT used in this work was substituted by a PMT with fast rise time.

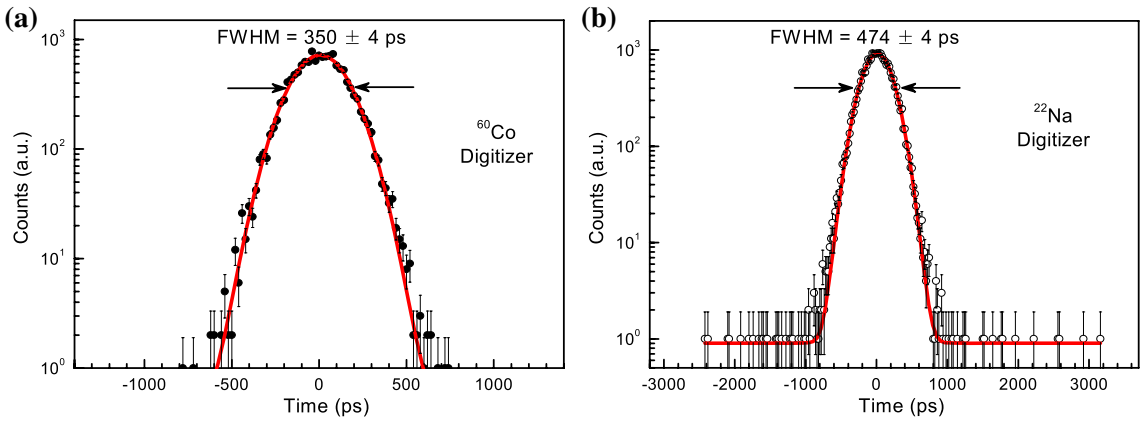

Fig. 11 Time resolutions for $CeBr_3$ 21# and 22#-HAMAMATSU PMT detectors in coincidence using the digital method. The FWHM resolutions are obtained assuming the two detectors have the same time characteristics. **a** ^{22}Na source; **b** ^{60}Co source

Table 4 Summary of time resolution for the $CeBr_3$-HAMAMATSU CR173-01 PMT at HV = 1050 V using sources of ^{60}Co (at 1173 keV/1332 keV) and ^{22}Na (at 511 keV)

Method	^{60}Co (ps)	^{22}Na (ps)
Analog	244 ± 2	336 ± 2
Digital	248 ± 3	335 ± 3

In order to demonstrate the fast timing characteristic of the $CeBr_3$ detectors, the half-life of ^{152}Sm 2^+ isomer was measured using the experiment system in this work with the similar method [15]. The result of 1.41 ± 0.02 ns is in excellent agreement with 1.428 ns from the *Table of Isotopes* [34].

Conclusions

In this work, the characteristics of two 1″ × 1″ $CeBr_3$-HAMAMATSU PMT detectors was investigated using both analog and digital methods. The results show that the time resolutions of the two $CeBr_3$ detectors are 244 ± 2 ps and 248 ± 3 ps at the energy peaks of ^{60}Co source, and 336 ± 2 ps and 335 ± 3 ps at 511 keV for the analog and the digital methods. As a result, the analog method can be substituted by digital method entirely based on a commercial digitizer, and the latter is more concise, efficiency and less expensive.

Due to the fast timing characteristic, $CeBr_3$ detector is a good option in the applications such as half-life measurements, ToF-PET and high counting rate conditions. Furthermore, it is a good γ-ray spectrometer owing to the preferable energy resolution and non-internal activity. It would be a strong competitor or substitute of the $LaBr_3$ detector which has the disadvantages of internal activity and costliness.

Funding This project was supported by the National Science Foundation of China (Grant No. 11575165 and 11775200).

References

1. C.W.E. van Eijk, Inorganic-scintillator development. Nucl. Instrum. Meth. A **460**, 1–14 (2001)
2. J. Marvin, Weber, Inorganic scintillators: today and tomorrow. J. Lumin. **100**, 35–45 (2002)
3. C.W.E. van Eijk, P. Dorenbos, E.V.D. van Loef et al., Energy resolution of some new inorganic-scintillator gamma-ray detectors. Radiat. Meas. **33**, 521–525 (2001)
4. S. Ra, S. Kim, H.J. Kim et al., Luminescence and scintillation properties of a CeBr 3 single crystal. IEEE T. Nucl. Sci. **55**, 1221–1224 (2008)
5. L. Trefilova, V. Cherginets, A. Gektin et al., The inertia properties of Cs2LiYCl6: Ce scintillation crystals. Radiat. Meas. **42**, 572–575 (2007)
6. E. Nácher, M. Martensson, O. Tengblad et al., Proton response of CEPA4: a novle LaBr 3(Ce)-LaCl3(Ce) phoswich array for high-energy gamma and proton spectroscopy. Nucl. Instrum. Methods A **769**, 105–111 (2015)
7. A. Gostojić, V. Tatischeff, J. Kiener et al., Characterization of LaBr 3: Ce and CeBr3 calorimeter modules for 3D imaging in gamma-ray astronomy. Nucl. Instrum. Meth. A **832**, 24–42 (2016)
8. A. Kozyrev, I. Mitrofanov, A. Owens et al., A comparative study of LaBr 3(Ce^{3+}) and CeBr3 based gamma-ray spectrometers for planetary remote sensing applications. Rev. Sci. Instrum. **87**, 085112 (2016)
9. A. Fabbri, D. Sacco, P. Bennati et al., Study of position reconstruction of a LaBr 3: Ce continuous scintillation crystal for medical applications. J. Instrum. **8**, 1–16 (2013)
10. L.M. Fraile, H. Mach, V. Vedia et al., Fast timing study of a CeBr 3 crystal: time resolution below 120 ps at 60Co energies. Nucl. Instrum. Meth. A **701**, 235–242 (2013)
11. F. Quarati, A.J.J. Bos, S. Brandenburg et al., X-ray and gamma-ray response of a 2″ × 2″ LaBr 3: Ce scintillation detector. Nucl. Instrum. Methods A **574**, 115–120 (2007)

12. F.G.A. Quarati, I.V. Khodyuk, C.W.E. van Eijk et al., Study of 138La radioactive decays using LaBr 3 scintillators. Nucl. Instrum. Methods A **683**, 46–52 (2012)
13. R. Billnert, S. Oberstedt, E. Andreotti et al., New information on the characteristics of 1 in × 1 in cerium bromide scintillation detectors. Nucl. Instrum. Methods A **647**, 94–99 (2011)
14. F.G.A. Quarati, P. Dorenbos, J. Van Der Biezen et al., Scintillation and detection characteristics of high-sensitivity CeBr 3 gamma-ray spectrometers. Nucl. Instrum. Methods A **729**, 596–604 (2013)
15. N. D'Olympia, S. Lakshmi, P. Chowdhury et al., Sub-nanosecond nuclear half-life and time-of-flight measurements with CeBr 3. Nucl. Instrum. Methods A **728**, 31–35 (2013)
16. F. Belli, B. Esposito, D. Marocco et al., A method for digital processing of pile-up events in organic scintillators. Nucl. Instrum. Methods A **595**, 512–519 (2008)
17. J. Pechousek, R. Prochazka, V. Prochazka et al., Virtual instrumentation technique used in the nuclear digital signal processing system design: energy and time measurement tests. Nucl. Instrum. Methods A **637**, 200–205 (2011)
18. B. Wan, X.Y. Zhang, L. Chen et al., Digital pulse shape discrimination methods for n-gamma separation in an EJ-301 liquid scintillation detector. Chin. Phys. C **11**, 116201.1–116201.5 (2015)
19. M. Nakhostin, A comparison of digital zero-crossing and charge-comparison methods for neutron/gamma-ray discrimination with liquid scintillation detectors. Nucl. Instrum. Methods A **797**, 77–82 (2015)
20. S.J. Asztalos, W. Hennig, W.K. Warburton, General purpose pulse shape analysis for fast scintillators implemented in digital readout electronics. Nucl. Instrum. Meth. A **806**, 128–132 (2016)
21. http,//www.hamamatsu.com.cn. Retrieved 21th Mar 2017
22. J.G. Qin, C.F. Lai, B.J. Ye et al., Characterizations of BC501A and BC537 liquid scintillator detectors. Appl. Radiat. Isotopes. **104**, 15–24 (2015)
23. W. Setyawan, R.M. Gaume, R.S. Feigelson et al., Comparative study of nonproportionality and electronic band structures features in scintillator materials. IEEE Trans. Nucl. Sci. **56**(5), 2989–2996 (2009)
24. V. Ivan, Khodyuk and Pieter Dorenbos, Trends and Patterns of Scintillator Nonproportionality. IEEE Trans. Nucl. Sci. **59**(6), 3320–3331 (2012)
25. A. Kozorezov, J.K. Wigmore, A. Owens, Picosecond dynamics of hot carriers and phonons and scintillator non-proportionality. J. Appl. Phys. **112**, 053079.1–053079.12 (2012)
26. Qi Li, Joel Q. Grim, R.T. Williams et al., A transport-based model of material trends in nonproportionality of scintillators. J. Appl. Phys. **109**, 123716.1–123716.17 (2011)
27. Pieter Dorenbos, Light output and energy resolution of Ce^{3+}-doped scintillators. Nucl. Instrum. Methods A **486**, 208–213 (2002)
28. L. Bardelli, G. Poggi, M. Bini et al., Time measurements by means of digital sampling techniques: a study case of 100 ps FWHM time resolution with a 100 Msample/s, 12 bit digitizer. Nucl. Instrum. Methods A **521**, 480–492 (2004)
29. P.A. Rodnyi, V.B. Mikhailik, G.B. Stryganyuk, Zimmerer. Luminescence properties of Ce-doped $Cs_2LiLaCl_6$ crystals. J. Lumin., **86**,161-166(2000)
30. Ulrich Ackermann, Werner Egger, Peter Sperr et al., Time- and energy-resolution measurements of BaF2, BC-418, LYSO and CeBr 3 scintillators. Nucl. Instrum. Meth. A **786**, 5–11 (2015)
31. A. Giaz, G. Hull, V. Fossati et al., Preliminary investigation of scintillator materials properties: SrI2:Eu, CeBr 3 and GYGAG: Ce for gamma rays up to 9 MeV. Nucl. Instrum. Meth. A **804**, 212–220 (2015)
32. Kanai S. Shah, Jaroslaw Glodo, William Higgins et al., CeBr 3 scintillators for gamma-ray spectroscopy. IEEE T. Nucl. Sci. **52**(6), 3157–3159 (2006)
33. L. Bardelli, M. Mini, G. Poggi et al., Application of digital sampling techniques to particle identification in scintillation detectors. Nucl. Instrum. Methods A **491**, 244–257 (2002)
34. Richard B. Firestone, Virginia S. Shirley, Coral M. Caglin et al., *Table of Isotopes*, Eighth Edition, Version 1.0 (Lawrence Berkeley National Laboratory, University of California, 1996), p.5755